FINAL REPORT

Title: Using Multi-scale Spatial Data to Improve Predictions of Immediate and Delayed Post-fire Mortality

JFSP PROJECT ID: 16-1-04-02

January 2021

James A. Lutz
Utah State University

Andrew J. Larson
University of Montana

Van R. Kane
University of Washington

Table of Contents

List of Tables

List of Figures

Abbreviations

LiDAR – Light detection and ranging
GIS – Geographic Information System
YFDP – Yosemite Forest Dynamics Plot
FOFEM – First Order Fire Effects Model
dNBR – differenced Normalized Burn Ratio
DBH – Diameter at Breast Height (1.37 m)
CVS – Crown Volume Scorched (%)
dNDVI – differenced Normalized Delta Vegetation Index
RdNBR – Relativized differenced Normalized Burn Ratio
RBR – Relativized Burn Ratio
TAO – Tree Approximate Object

Keywords

Fire effects, fire ecology, surface fuel, forest structure, landscape pattern, Smithsonian ForestGEO, spatial pattern, Yosemite Forest Dynamics Plot, Yosemite National Park

Acknowledgements

We thank the field technicians and volunteers who assisted with field measurements at the Yosemite Forest Dynamics Plot, each of whom is acknowledged at http://yfdp.org. We thank the managers and staff of Yosemite National Park for their logistical assistance and support. We thank the Ecology Center and the Utah State Agricultural Experiment Station at Utah State University which also supported this project.

Abstract

Fires are increasingly large, and our understanding of their effects inherently depends on spatial scale. At small scales, heterogeneity of fuels and consumption is large. At landscape scales our understanding is necessarily based on remotely sensed data, and from models developed from study plots. We examined the effects of the California Rim Fire of 2013 on tree mortality at scales from 1 m^2 to 50,000 ha in Yosemite National Park. Our objectives were to:

- Quantify the effect of tree spatial neighborhood on the probability of immediate and delayed fire mortality using mapped tree locations.
- Determine the correlation between satellite-derived fire severity and actual tree mortality, including quantification of uncertainties.
- Quantify the effect of tree spatial neighborhood on the probability of immediate and delayed fire mortality using airborne LiDAR-derived Tree Approximate Objects (TAOs).

The most widely used mortality model, FOFEM, may not be suitable to predict post-fire mortality of hardwood species or large-diameter trees. Background mortality agents (i.e., bark beetles) and dense tree neighborhoods can increase probability of mortality, and this can result in patches of elevated mortality. Spatial metrics can be incorporated into mortality models to improve accuracy. Climate effects were pronounced for large-diameter trees which can be more susceptible to bark beetle-caused post-fire mortality. Satellite-derived fire severity maps may reflect broad-scale patterns in severity but should not be treated as absolute truth with respect to actual tree mortality on a stem or biomass basis. Uncertainty may be reduced by supplementing severity maps with field-based observations of fire effects. Smaller trees mostly died either in the fire or soon thereafter and larger trees died in later years. Mortality predictors at the TAO scale fell into categories of fuel connectivity, fire tolerance, and local stress. These three categories acted as a series of filters determining whether a tree escaped fire damage, died immediately, died 2-4 years post-fire, or recovered. The first filter had to do with loads and spatial configurations of surface and understory fuels, ladder fuels, and horizontal canopy fuel breaks: trees in areas of lower fuel connectivity were more likely to survive. The second filter was fire tolerance, which allowed larger trees and more fire tolerant species to resist immediate fire-caused mortality. Lastly, local stress conditions predicted the amount of delayed mortality. Including cross-scale linkages between neighborhood-level and TAO-level substantially improved models, aligning with the theoretical understanding of fire's landscape ecology, where different scales rest within a hierarchical structure with cross-scale interactions.

This study achieved an important step forward in the development of a theory of landscape fire ecology with practical applications for land managers. By scaling from individual stems to large landscapes using a fusion of field-based individual tree data, high-resolution LiDAR data, and satellite derived fire severity maps, we showed that that formalizing the hierarchical structure of landscapes in empirical models is a productive way to advance the understanding of disturbance processes in a manner informative to management planning and post-fire response.

The establishment of the Yosemite Forest Dynamics Plot, and its subsequent burning by the Rim Fire, enabled us to leverage a decade of annual tree mortality measurements among 43,937 trees, snags, and logs to evaluate fire science tools in novel ways. The post-fire research we conducted with this unique dataset is a powerful complement to previous studies based on more traditional sampling designs, making this body of research a critical contribution to the field of fire ecology.

Objectives

Natural resource managers need to have accurate models of fire mortality that consider both prompt and delayed effects. This project determined that revisions of models to include density-dependence in post-fire tree mortality modeling is warranted. With revised models, managers would have improved ability to extrapolate model results over management units that can have heterogeneous tree densities and basal areas. This project used new methods of fusing Landsat and LiDAR data to extrapolate mortality predictions across landscapes.

1. Project Objectives & Hypotheses

Objective 1: Quantify the effect of tree spatial neighborhood on the probability of immediate and delayed fire mortality using mapped tree locations. We hypothesized that trees closer together (i.e., in clumps) would share similar fates – that they would be either more likely to experience fire mortality than average for the stand (i.e., small group torching) or less likely to experience fire mortality, but not the average. We further hypothesized that delayed fire mortality (post-fire years 2-5) would be spatially aggregated and density-dependent, as the contributing factors (i.e., bark beetles, fungi, competition) are aggregated, and because they often act in a density-dependent fashion (e.g., Negrón and Popp 2004).

Objective 2: Determine the correlation between satellite-derived fire severity and actual tree mortality, including quantification of uncertainties introduced by Landsat scene positions. We examined common and emerging spectral indices of vegetation change due to fire; the differenced Normalized Delta Vegetation Index (dNDVI; Tucker 1979), the differenced Normalized Burn Ratio (dNBR; Key and Benson 2006), the Relativized differenced Normalized Burn Ratio (RdNBR; Miller and Thode 2007), and the Relativized Burn Ratio (RBR; Parks *et al.* 2014). We also performed a literature search and examined all less commonly used vegetation indices used for fire based on Landsat data.

Objective 3: Quantify the effect of tree spatial neighborhood on the probability of immediate and delayed fire mortality using LiDAR-derived Tree Approximate Objects (TAOs). Objective #3 examined whether any improvement in mortality predictions using the tree stem map (Objective #1) can be extended to the broader landscape without the full information about tree positions in stem map data.

Deliverables Summary

This project produced seven peer-reviewed publications, two dissertations, nine presentations, two open access data sets, one field and database protocol document, one outreach document and a project webpage. Data collection, data analysis, publication of research results and conclusions, and open access data publication are complete. All objectives were met. Research objectives were analyzed more comprehensively than originally proposed, and deliverables exceeded plan (Table 4). The peer-reviewed publications have been cited 69 times as of 2/1/2021, and the data publications are in use by USFS investigators. This report summarizes our findings, with full details in the publications uploaded to the JSFP reporting portal.

Background

Density-dependent mortality—the situation in which probability of mortality is higher in local areas of high tree density—is one of the most universal ecology concepts guiding forest management. Stand dynamics theory (Oliver and Larson 1996), numerous recent empirical tree mortality studies (e.g., Das *et al.* 2011), including those of post-fire tree mortality (Yu *et al.* 2009), and the forest entomology literature (e.g., Negrón and Popp 2004) all emphasize that local crowding increases the likelihood of tree death. **Yet, the post-fire tree mortality equations used in common modeling platforms (e.g., FOFEM; Lutes 2014) do not include terms for local crowding, and density-dependence was not considered when those mortality models were developed (Ryan and Reinhardt 1988, Hood *et al.* 2010).** This raises the question as to whether current models are comprehensive and fully appropriate, especially in forests with heterogeneous tree densities or heterogeneous burn severities. Mangers need models that work across the spectrum of pre-fire and post-fire conditions to credibly guide decisions about post-fire landscape management, which highlights the need to rigorously evaluate current models. **We will evaluate existing models of post-fire tree mortality to determine the potential improvement in accuracy offered by incorporating information about local tree neighborhood density.**

Despite the increasing magnitude of tree mortality (e.g., van Mantgem *et al.* 2013) and the importance of post-fire refugia for forest regeneration (e.g., Kolden *et al.* 2012), the spatial distribution of fire mortality remains understudied. When spatial patterns of fire mortality are considered, they are usually inferred from Landsat-derived spectral changes (e.g., van Wagtendonk and Lutz 2007) at a 900 m^2 grain. While landscape scale fire mortality has been inferred from these satellite-derived metrics, fire severity is approximated using correlations with ground measurements that include no explicit spatial information (i.e., Composite Burn Index plots; CBI [Key and Benson 2006]) and broad categories of trees (e.g., big trees, intermediate trees) rather than actual tree species and sizes. And despite the wide use of satellite-derived spectral indices, no one has yet quantified the precise tree death that is associated with Landsat-derived spectral changes. The ambiguities in interpreting tree mortality from spectral changes between pre-fire and post-fire images, including the various combinations of individual tree mortality that can lead to similar spectral changes, and the sensitivities of Landsat-derived fire severity values to location uncertainties of Landsat pixels (Storey *et al.* 2014) remain serious barriers to more effective use of available satellite data (e.g., Monitoring Trends in Burn Severity, MTBS, Eidenshink *et al.* 2007).

The reason that spatially explicit post-fire mortality has been understudied is the requirement for a study site of sufficient size where the trees and fuel have been mapped pre-fire, where the data are not lost during the fire, and where measurements of tree mortality (or survival) are repeated post-fire. Examining spatial neighborhoods of tree mortality requires large, mapped plots, almost certainly >1 ha (Das *et al.* 2011), with sizes ≥10 ha (Lutz *et al.* 2014) more likely to produce meaningful results. Furthermore, to infer statistically significant relationships between tree mortality and Landsat data would require hundreds of contiguous Landsat pixels within which the trees were all mapped.

We propose to address these issues with a unique, matched set of pre-fire and post-fire data – a 25.6 ha plot (800 m × 320 m; $^1/_2$ mile × $^1/_5$ mile) where all 34,579 trees have been mapped and tracked from three years before the Rim Fire to two years post-fire and will be

tracked over the course of this proposal to five years post-fire. This plot contains 238 contiguous Landsat pixels and experienced 24,319 immediate fire mortalities, with 7,408 trees surviving two years post-fire. The spatial scale of the plot and the matched set of pre-fire and post-fire data were collected to specifically examine the scale of fire effects in mixed-conifer forests. This unparalleled field dataset is enhanced by matched high resolution (40 pulses m^{-2}) LiDAR data collected pre-fire, providing opportunities to extrapolate our results over large landscapes. This study site offers perhaps the best opportunity in the world today to examine the spatial aspects of prompt and delayed fire mortality and evaluate existing tree mortality models.

Study Area and Report Organization

The study area comprises the forested portion of Yosemite National Park burned by the 2013 Rim Fire and covered by pre-fire LiDAR (Fig. 1). We used pre-fire and post-fire data from the Yosemite Forest Dynamics Plot and 53, 0.25-ha validation plots that we installed as part of this research to address the research questions. We have summarized each research objective in its own section (the definitive methods and results are contained within the resulting peer-reviewed publications, uploaded to the JSFP web portal). We also provide an addition section detailing the syntheses we were able to perform in addition to the original project scope.

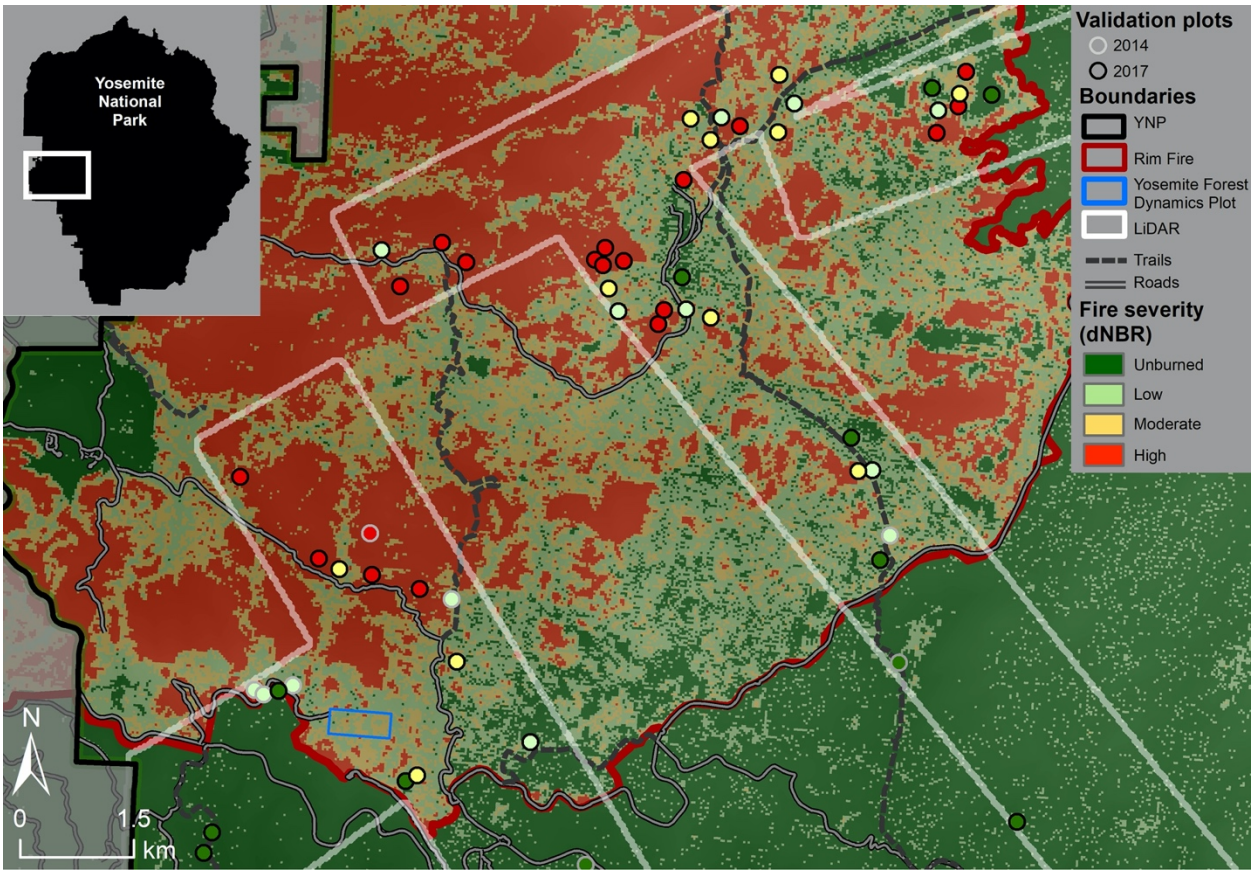

Fig. 1. Location of the portion of the 2013 Rim Fire within Yosemite National Park including the primary study site (the Yosemite Forest Dynamics Plot) and the 53 validation plots established throughout the Rim Fire footprint.

The Yosemite Forest Dynamics Plot experienced a moderate level of direct fire mortality in the Rim Fire (Fig. 2). However, the subsequent and persistent drought brought heightened levels of post-fire delayed tree mortality.

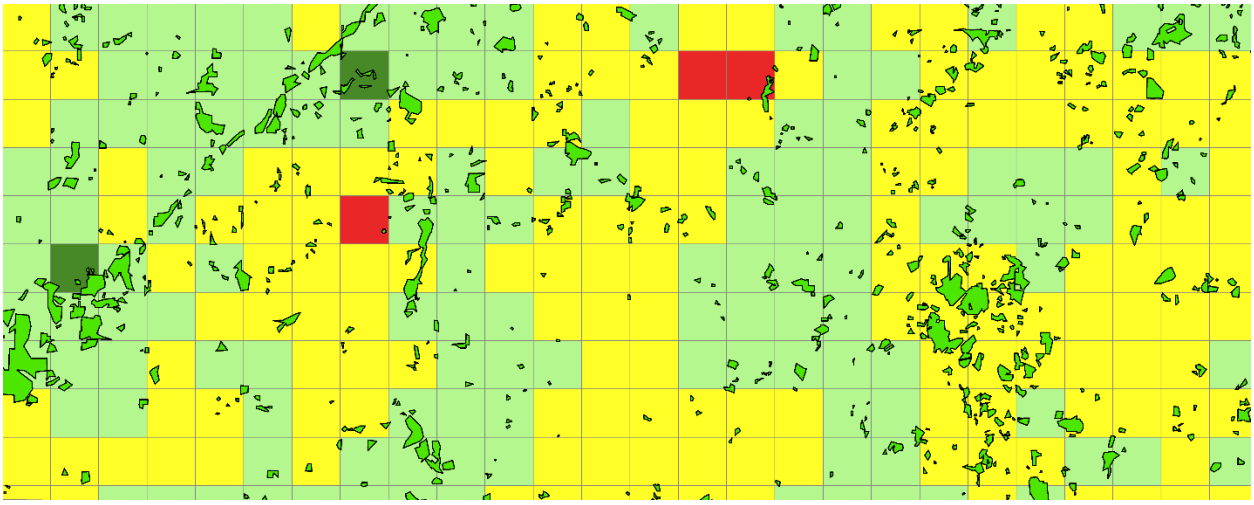

Fig. 2. Landsat-derived fire severity within the Yosemite Forest Dynamics Plot (YFDP; 800 m × 320 m; $^1/_2$ mile × $^1/_5$ mile) showing differenced Normalized Burn Ratio severities. Irregular medium green patches are surface areas that did not burn in the Rim Fire (Blomdahl et al. 2019). The 53 validation plots (Fig. 1) were selected to complement the severity distribution in the YFDP.

Objective 1: Effects of Tree Spatial Neighborhood on Mortality

Key Publications

Furniss, T. J., A. J. Larson, V. R. Kane, and J. A. Lutz. 2020. Wildfire and drought moderate the spatial elements of tree mortality. *Ecosphere*. 11(8): e03214. https://doi.org/10.1002/ecs2.3214

Furniss, T. J., A. J. Larson, V. R. Kane, and J. A. Lutz. 2019. Multi-scale assessment of post-fire tree mortality models. *International Journal of Wildland Fire* 28(1): 46-61. https://doi.org/10.1071/WF18031 **Editor's Choice.**

Research Questions

1) To what extent do fine-scale ecological factors (i.e., tree neighborhoods, topography, soils) influence predictive accuracy of post-fire mortality models?
2) Are post-fire mortality models suitable to predict mortality of large-diameter trees?
3) Do local tree neighborhoods moderate post-fire tree mortality, and if so, at what scales?
4) How do background mortality processes, such as pests, pathogens, and competition, mediate the spatial pattern of post-fire mortality?

Methods

We evaluated the performance of mortality models within the First Order Fire Effects Model (FOFEM) software, and compared their performance to locally-parameterized models based on five different model formulae. We evaluated all models at the individual tree and stand levels with the YFDP dataset comprising 34 174 trees. We compared stand-level accuracy across a range of spatial scales, and we used point pattern analysis to test the accuracy with which mortality models predict post-fire tree spatial pattern.

We assessed the role of background mortality processes in moderating patterns of post-fire mortality by measuring the rates, causes, and spatial pattern of mortality annually for 3 years pre-fire and 5 years post-fire. We characterized the relationships between background mortality, compound disturbances (fire and drought), and forest spatial structure using generalized linear models and spatial point pattern analysis. We integrated our findings with a synthesis of the existing literature and developed a conceptual framework describing the spatio-temporal signatures of background and disturbance-related tree mortality.

Key Findings

FOFEM under-predicted mortality for conifers (Fig. 3), possibly because of the timing of the Rim Fire during a severe multi-year drought. Models based on crown scorch were most accurate in predicting individual tree mortality, but tree diameter-based models were more accurate at the stand level for *Abies concolor* and large-diameter *Pinus lambertiana* – the most abundant species in this forest. Stand-level accuracy was reduced by spatially correlated error at small spatial scales, but stabilized at scales ~1 ha. The predictive error of FOFEM generated inaccurate predictions of post-fire spatial pattern at small scales, and this error could be reduced by improving FOFEM model accuracy for small trees.

Background mortality processes interacted with fire and drought to alter the rate, spatial pattern, and ecological consequences of mortality (Fig. 4). Before fire, spatially non-random mortality was only evident among small ($1 < \text{cm DBH} \leq 10$) and medium ($10 < \text{cm DBH} \leq 60$) diameter

classes; mortality rates were low (1.7% yr^{-1}), and mortality was density-dependent among small-diameter trees. Direct fire damage caused the greatest number of moralities (70% of stems ≥1 cm DBH), but the more enduring effects of this disturbance on the demography and spatial pattern of large-diameter trees occurred during the post-fire mortality regime (Fig. 4). The combined effects of disturbance and biotic mortality agents provoked density-dependent mortality among large-diameter (≥60 cm DBH) trees, eliciting a distinct post-disturbance mortality regime that did not resemble the pattern of either pre-fire mortality or direct fire effects. The disproportionate ecological significance of the largest trees renders this mortality regime acutely consequential to the long-term structure and function of forests.

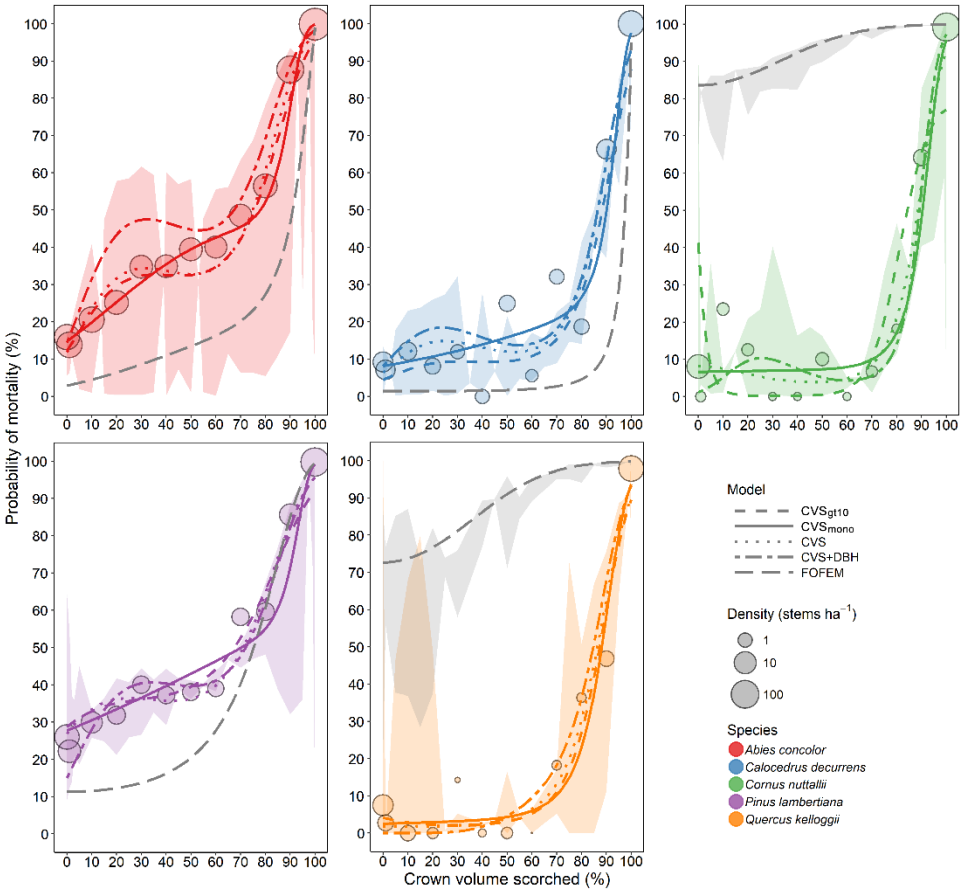

Fig. 3. Probability of mortality (Pm) as a function of crown volume scorched (CVS). Dots represent observed proportion of stems that were killed in each CVS category (10% bins plus 0% and 100% bins), and lines represent species-specific logistic regression models using CVS as the independent variable and binary mortality status as the response. The dots are for visualization purposes only; the models were parameterized on rarefied, unbinned data. For the CVS þ DBH and FOFEMRA models, shaded areas represent the full range of modelled Pm values (CVS þ DBH colored (light grey in greyscale version), FOFEMRA in grey (dark grey in greyscale version)), whereas the dotted lines represent Pm while DBH was held constant (using average DBH).

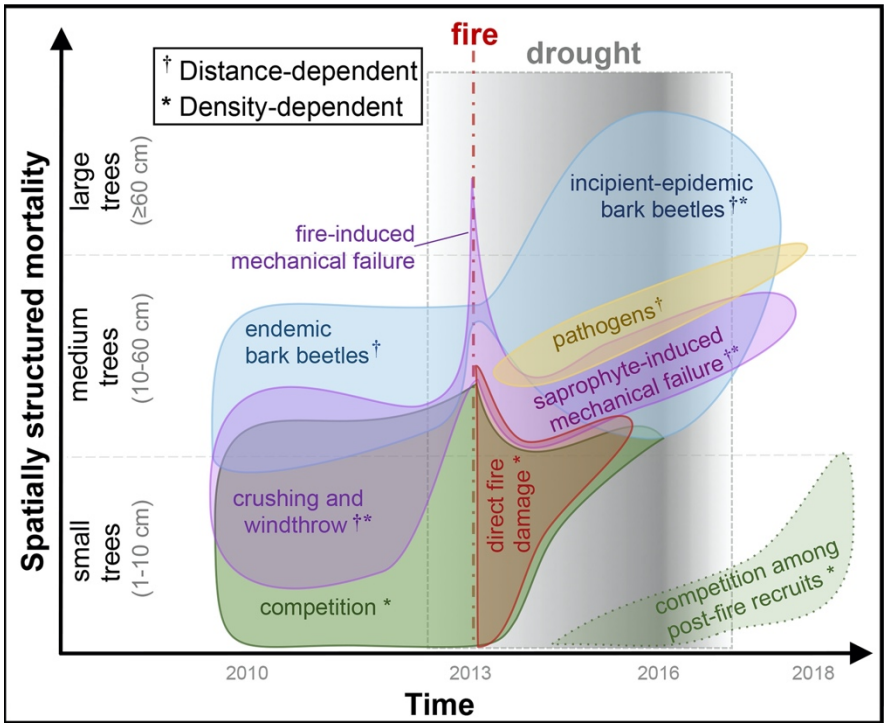

Fig. 4. Empirically informed conceptual model describing the development of spatially structured mortality processes before, during, and after compound disturbance (fire and drought). Polygons represent different mortality agents (colors match with Fig. 1). Position along the y-axis represents the tree diameters (cm DBH) for which each mortality process was spatially structured. The strength of each process (as detected in this study) is approximately related to polygon size. Superscripts indicate the form of spatial structuring (distance and/or density dependence) that was most evident for each process. Competition among post-fire recruitment was not analyzed in this study but is shown in its hypothesized position.

Objective 2: Satellite Measurement of Actual Tree Mortality

Key Publication

Furniss, T. J., V. R. Kane, A. J. Larson, and J. A. Lutz. 2020. Detecting actual tree mortality with satellite-derived spectral indices and estimating landscape-level uncertainty. *Remote Sensing of Environment* 237: 111497. https://doi.org/10.1016/j.rse.2019.111497

Research Questions

1) How much uncertainty in tree mortality (field-based measurements of stem density and basal area) should be expected across a continuum of satellite-derived spectral index values?
2) Which spectral indices have the highest accuracy for those field-based tree mortality metrics (i.e., basal area of mortality, percent change in density, and mortality of large-diameter trees), and what is the range of fire severity for which accuracy is highest?
3) How can variability in satellite-derived estimates of observed mortality may be scaled up to assess uncertainty in tree mortality and patch metrics at the landscape scale (>1000 km^2)?

Methods

We used the YFDP dataset in conjunction with an auxiliary dataset of 53 0.25-ha stem-mapped plots (Fig. 1) to quantify fire severity using field-based measurements of fire effects (mortality-induced change in stem density and basal area). We used the geo-referenced the location of each tree within each plot, and we grouped trees into units based on 30-m Landsat pixels. We treated each pixel within the YFDP and each of the 53 0.25-ha plots as separate sample units, and we correlated spectral index value to actual tree mortality. We used generalized linear models and Random Forest to evaluate the strength of the correlation between satellite- and field-based severity metrics. We used these correlations to impute minimum, maximum, and mean tree mortality within each 30-m pixel for the entire Rim Fire footprint.

Landsat 8 scenes were chosen to maximize scene clarity while matching pre- and post-fire phenology, and we conducted a phenological offset calibration to minimize the difference in phenology between the two scenes. Images were terrain corrected and co-registered by the USGS Earth Resources Observation and Science Center (EROS). These orthorectified top-of-atmosphere reflectance images were further processed by USGS EROS to remove atmospheric effects, resulting in Level-2 surface reflectance (SR) image products that were accessed through the EROS Science Processing Architecture bulk ordering service (https://espa.cr.usgs.gov). We compiled a list of 36 spectral indices that are sensitive changes in vegetation, with an emphasis on indices that have been used to detect fire effects (Table 2).

Table 1. Satellite-derived spectral indices and topographic variables. Subscripts 'pre' and 'post' indicate pre-fire and post-fire; L8 stands for Landsat 8; 'R' stands for spectral wavelengths within the red band, 'G' for the green band, 'B' for the blue band, 'NIR' for the near-infrared band, 'SWIR1' for the shortwave infrared band centered at 1.6 μm, and 'SWIR2' for the shortwave infrared band centered at 2.2 μm. Wavelength thresholds for each band may be found in the Landsat 8 handbook.

	Index	Code	Formula (L8)	Citation
Snapshot	Normalized differenced vegetation index	NDVI	(NIR - Red) / (NIR + Red)	Rouse et al. 1974; Tucker 1979
	Mid-IR bispectral index	MIRBI	10*SWIR2 - 9.8*SWIR1 + 2	Trigg and Flasse 2001
	Normalized burn index	NBR	(NIR - SWIR2) / (NIR + SWIR2)*1000	Key and Benson 2006
	Char soil index	CSI	NIR / SWIR1	Smith et al. 2007
	Soil-adjusted vegetation index	SAVI	((NIR - Red) * (1.0 + *L*)) / (NIR + Red + *L*)	Huete 1988; Barbosa et al. 1999
	Normalized differenced moisture index	NDMI	(NIR - SWIR1) / (NIR + SWIR1)	Wilson & Sader 2002; Gao 1996
	SWIR1 to NIR ratio	SWIR1:NIR	SWIR1 / NIR	Vogelmann 1990
	SWIR2 to NIR ratio	SWIR2:NIR	SWIR2 / NIR	Kushla and Ripple 1998
	SWIR2 to SWIR1 ratio	SWIR2:SWIR1	SWIR2 / SWIR1	Epting et al. 2005
	NIR to G ratio	NIR:G	NIR / G	Landsat 8 handbook
	NIR to R ratio	NIR:R	NIR / R	Landsat 8 handbook
	Tassled-cap brightness	TC.BRI	∑(coefficients * L8 bands 2 to 7)	Baig et al. 2014
	Tassled-cap greeness	TC.GRE	∑(coefficients * L8 bands 2 to 7)	Baig et al. 2014
	Tassled-cap wetness	TC.WET	∑(coefficients * L8 bands 2 to 7)	Baig et al. 2014
Bi-temporal	Differenced individual bands	dB	B_{pre} - B_{post}	McCarley et al. 2017
		dG	G_{pre} - G_{post}	McCarley et al. 2017
		dR	R_{pre} - R_{post}	McCarley et al. 2017
		dNIR	NIR_{pre} - NIR_{post}	McCarley et al. 2017
		dSWIR1	$SWIR1_{pre}$ - $SWIR1_{post}$	McCarley et al. 2017
		dSWIR2	$SWIR2_{pre}$ - $SWIR2_{post}$	McCarley et al. 2017
	Differenced indices	dNDVI	$NDVI_{pre}$ - $NDVI_{post}$	Meddens et al. 2016, McCarley et al. 2017
		dMIRBI	$MIRBI_{pre}$ - $MIRBI_{post}$	McCarley et al. 2017, 2018
		dNBR	NBR_{pre} - NBR_{post}	Key and Benson 2006
		RdNBR	dNBR / $(\lvert NBR_{pre}\rvert / 1000)^{0.5}$	Miller and Thode 2007
		RBR	dNBR / (($\lvert NBR_{pre}\rvert$ / 1000) + 1.001)	Parks et al. 2014
		dCSI	CSI_{pre} - CSI_{post}	Smith et al. 2007
		dSAVI	$SAVI_{pre}$ - $SAVI_{post}$	McCarley et al. 2017
		dNDMI	$NDMI_{pre}$ - $NDMI_{post}$	Meddens et al. 2016, McCarley et al. 2017
	Differenced band ratios	dSWIR1:NIR	$SWIR1.NIR_{pre}$ - $SWIR1.NIR_{post}$	Meddens et al. 2016
		dSWIR2:NIR	$SWIR2:NIR_{pre}$ - $SWIR2:NIR_{post}$	McCarley et al. 2017
		dSWIR2:SWIR1	$SWIR2:SWIR1_{pre}$ - $SWIR2:SWIR1_{post}$	McCarley et al. 2017
		dNIR:G	$NIR:G_{pre}$ - $NIR:G_{post}$	This study
		dNIR:R	$NIR:R_{pre}$ - $NIR:R_{post}$	This study
	Differenced tassled-cap	dTC.BRI	$TC.BRI_{pre}$ – $TC.BRI_{post}$	Meddens et al. 2016, McCarley et al. 2017
		dTC.GRE	$TC.GRE_{pre}$ – $TC.GRE_{post}$	Meddens et al. 2016, McCarley et al. 2017
		dTC.WET	$TC.WET_{pre}$ – $TC.WET_{post}$	Meddens et al. 2016, McCarley et al. 2017

Key Findings

Contrary to recent developments in relativized severity metrics, we did not find that these relativized versions of dNBR (RBR and RdNBR) consistently improved accuracy. This is likely related to the spatial scope of this study, and relativization may still be more important for examining regional trends in fire severity across multiple fire seasons. No single severity index was most accurate for all field-based severity metrics; dNDVI was best for density-based metrics of mortality while dNBR performed better for basal area-based metrics.

We found a high degree of variability in actual tree mortality that was indistinguishable based on satellite-derived severity indices; satellite-derived fire severity metrics are imprecise gauges of actual tree mortality (Fig. 5). Importantly, this variability was highest at intermediate fire severities. This translated into a considerable amount of uncertainty at the landscape scale, with an expected range in estimated percent basal area mortality greater than 37% for half of the area burned (>50,000 ha). In other words, a 37% range in predicted mortality rate was insufficient to capture the observed mortality rate for half of the area burned (Fig. 6). Uncertainty was even greater for percent stem mortality, with half of the area burned exceeding a 46% range in predicted mortality rate. The high degree of uncertainty in tree mortality that we observed challenges the confidence with which Landsat-derived spectral indices have been used to measure fire effects, and this has broad implications for research and management related to post-fire landscape complexity, distribution of seed sources, or persistence of fire refugia.

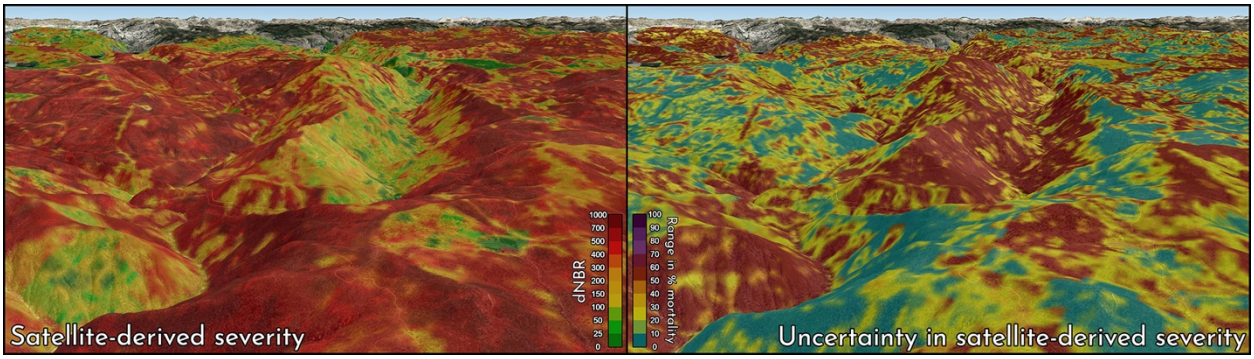

Fig. 5. Uncertainty in satellite-derived fire severity. These 3D images were generated in Google Earth with raster overlays (see Fig. 6).

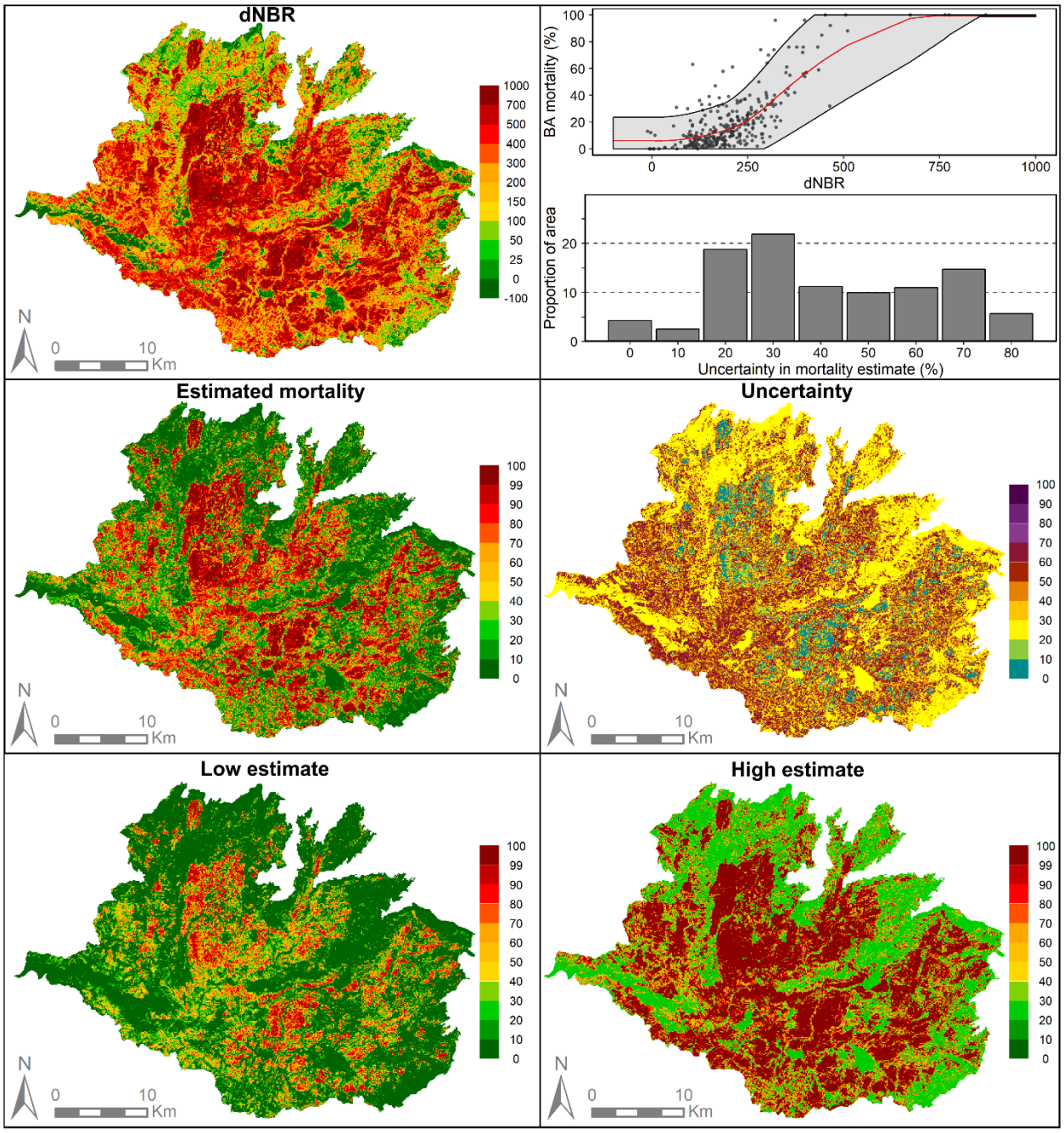

Fig. 6. Estimation of actual tree mortality based on the differenced Normalized Burn Ratio (dNBR).

Objective 3: Use of LiDAR to Predict Tree Mortality

Key Publication

Jeronimo, S. M. A., J. A. Lutz, V. R. Kane, A. J. Larson, and J. F. Franklin. 2020. Burn weather and three-dimensional fuel structure determine post-fire tree mortality. *Landscape Ecology* 35: 859-878. https://doi.org/10.1007/s10980-020-00983-0

Research Questions

1. How does tree mortality progress 1–4 years post-fire in terms of mortality rates and demographics?
2. What elements of vertical forest structure and horizontal pattern predict immediate and delayed post-fire tree mortality at scales from small groups of trees to larger neighborhood patches?
3. Are there interactions between effects at different scales, and are those interactions directional (i.e., broader to finer scales or finer to broader scales)?
4. How does the prevalence of different mortality agents vary with changes in fine-scale predictors of post-fire tree mortality?

Methods

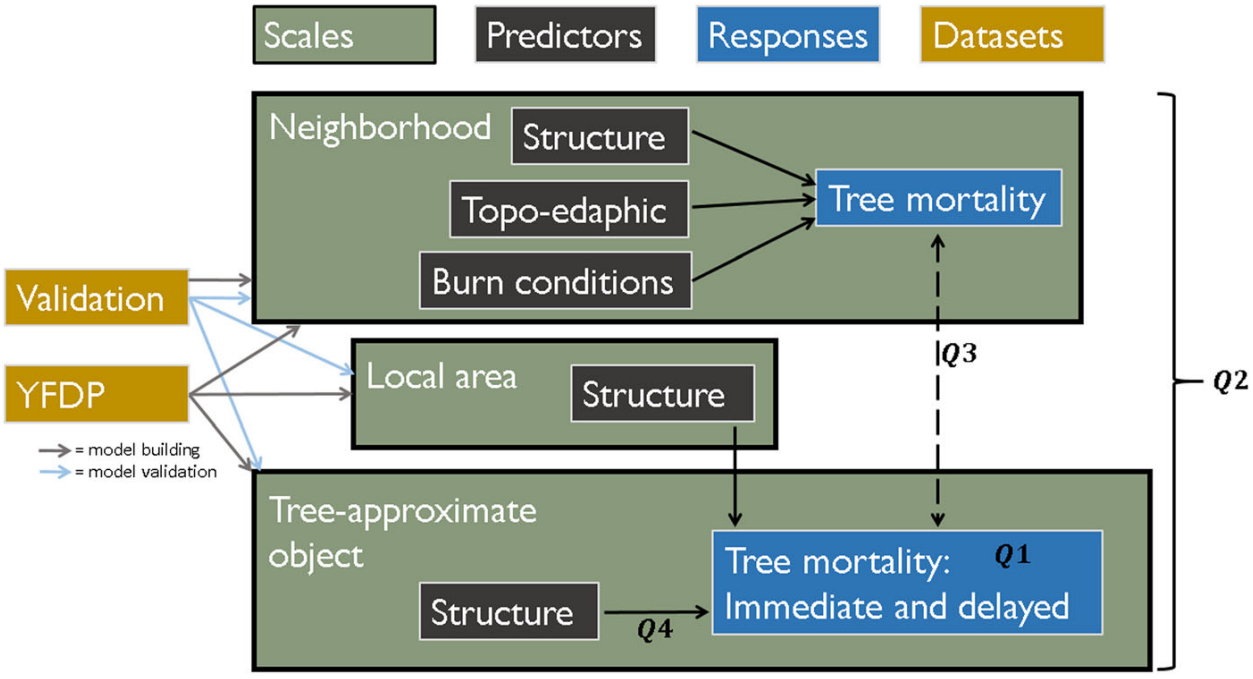

Fig. 7. Flowchart of data sources, conceptual formulation of mortality model, and relationships to study questions, In the model schematic, black arrows represent explanatory variables being used to predict a response variable, while the dashed arrow between response variables represents an explicitly modeled cross-scale interaction. Models were tested both with and without this term. Labels Q1-Q4 represent the four study questions: labels are placed next to the data source, interaction, or model analyzed to answer each question.

We answered the research questions using direct analysis of field and remote sensing data, along with a post-fire mortality model built using these data (Fig. 7).

To answer question 1, we analyzed annual post-fire mortality data from the YFDP from 2014-2017. We assessed year-on-year mortality rates, the share of mortality which occurred in each year, and the average diameter of new mortalities for each year.

To answer questions 2 and 3, we created a hierarchical model to predict field-measured post-fire tree mortality from pre-fire remotely sensed forest structure and pattern measurements. We computed predictor variables at three scales for both the YFDP and 48 of the 53 validation plots: tree-approximate object (TAO), a 0.1 ha local area centered on each TAO, and fixed 90 × 90 m neighborhoods. TAOs represent objects resolvable by lidar, each of which is a canopy tree along with any subordinate trees that may be hidden by the dominant tree's foliage. We subdivided the YFDP into 24 neighborhoods containing 1,773 TAOs and their associated local areas. Each validation plot represented one neighborhood, and the 48 plots contained a total of 847 TAOs with associated local areas. We calculated a variety of structure and pattern metrics from lidar for each unit of measurement (Table 2). At the neighborhood scale, we additionally included water balance and burn weather predictors (Table 2).

We computed model response variables at the neighborhood and TAO scales based on field data. At the neighborhood scale the response variable was total mortality rate within the neighborhood. At the TAO scale the response variable was the number of trees in each of the following categories: immediate mortality (dead by 2014 survey), delayed mortality (dead by 2017 survey), and survival (alive during 2017 survey).

We used the YFDP data to build the TAO-scale models, retaining the validation plots as an independent testing dataset. For the neighborhood-scale models, we also used the validation plots as training data in order to capture a wider range of environmental and burning conditions.

We analyzed four sets of models, which were factorial combinations of including vs excluding the water balance and burn weather predictors and treating the TAO scale as explicitly nested within the neighborhood scale vs independent models at the two scales. To answer question 2, we used an objective variable selection method, calculated variable importance values, and evaluated the sign of fitted coefficients for each predictor variable. To answer question 3, we calculated model assessment statistics for each of the four tested models and evaluated the effect of explicitly including the scale hierarchy in the model formulation.

To answer question 4, we investigated relationships between the most important predictor variables and causes of post-fire tree mortality. We identified critical thresholds of the important predictors that best differentiated between different causes of mortality, then summarized field-identified mortality factors above and below those thresholds.

Table 2 Predictors selected for the final models, importance values, and signs of predictor relationships to mortality and survival. I = immediate, D = delayed, S = survival.

	Predictor	**Importance value**	**Sign**		
Sub-model	Actual evapotranspiration (mm H_2O yr^{-1})	1.00	+		
	Open space (proportion)	1.00	–		
	Energy release component (BTU ft^{-2})	0.99	–		
	Maximum burn day temperature (°C)	0.96	+		
	Canopy cover >2 m (%)	0.88	+		
	Rumple (m^2 m^{-2})	0.80	+		
			I	**D**	**S**
TAO immediate mortality	Maximum height (m)	1.00	–	+	+
	Canopy cover <8 m (%)	1.00	+	–	–
	Mean clump size in local area (*n* TAOs)	0.99	+	–	–
	Local area open space (%)	0.89	–	–	+
	Leaf area index (m^2 m^{-2})	0.73	+	+	–
TAO delayed mortality	Local density (TAOs ha^{-1})	1.00	+	+	–
	Canopy cover 8-16 m (%)	0.99	–	+	+
	Canopy cover < 2 m (%)	0.99	+	–	–
	Crown fuel weight (kg)	0.88	–	–	+
	Crown base height (m)	0.86	–	+	+

Key Findings

The Rim Fire exhibited generally characteristic severity throughout Yosemite National Park (Figs. 1, 2) which translated into moderate mortality rates (Fig. 8).

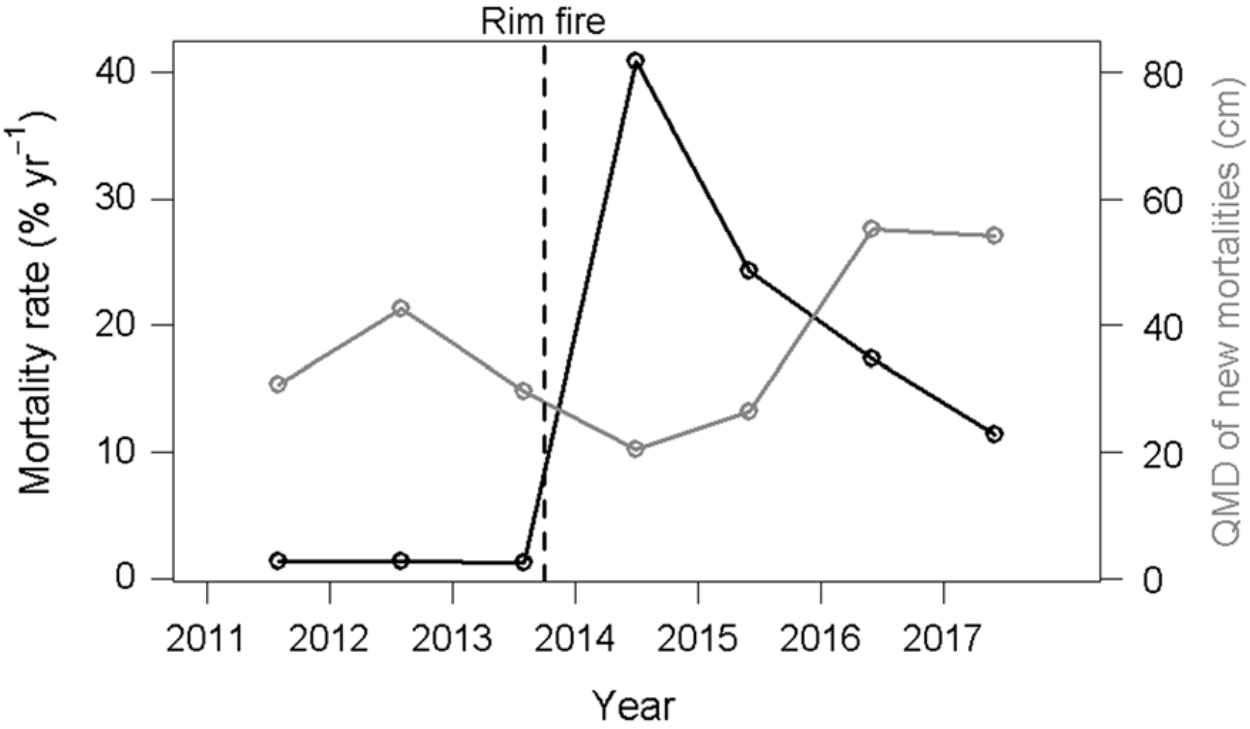

Fig. 8. Rates and demographics of tree mortality for trees ≥10 cm dbh on the YFDP for three pre-fire censuses and four post-fire censuses. QMD = quadratic mean diameter.

Question 1

Of trees ≥10 cm dbh that were alive in 2013 (n = 11,974), 39% died immediately after fire, 24% died 2-4 years post-fire, and the remaining 37% were alive in May 2017. Mortality decreased over time: 62% of mortalities occurred in the first year (2013-2014) followed by 22% in the second year, 12% in the third year, and 4% in the fourth year. Mortality rates decreased similarly, with a rate of 39% the first year, 23% of remaining live trees the second year, 16% the third year, and 6% the fourth year (Fig. 8). In general, smaller trees died either in the fire or soon thereafter and larger trees died in later years (Fig. 8).

Question 2

The neighborhood-scale mortality predictors fell into three categories: fuel amounts, fuel configuration, and burn weather (Table 2). Topographic predictors like slope and topographic position were not themselves important predictors, but do affect water balance, suggesting that the importance of topography was mainly expressed through its role in modulating growing conditions, and that the influence of burn weather on fire severity was greater than the influence of topography.

Mortality predictors at the TAO scale fell into categories of fuel connectivity, fire tolerance, and local stress (Fig. 9). Conditions in these categories acted as a series of filters determining whether a tree escaped fire damage, died immediately, died 2-4 years post-fire, or recovered. The

first filter of important predictors had to do with loads and spatial configurations of surface and understory fuels, ladder fuels, and horizontal canopy fuel breaks: trees in areas of lower fuel connectivity were more likely to survive. The second filter was fire tolerance, which allowed larger trees and more fire tolerant species to resist immediate fire-caused mortality. Lastly, local stress conditions predicted the amount of delayed mortality. Trees in lower density areas and with larger crowns were subject to less stress and thus more likely to recover from fire effects without dying.

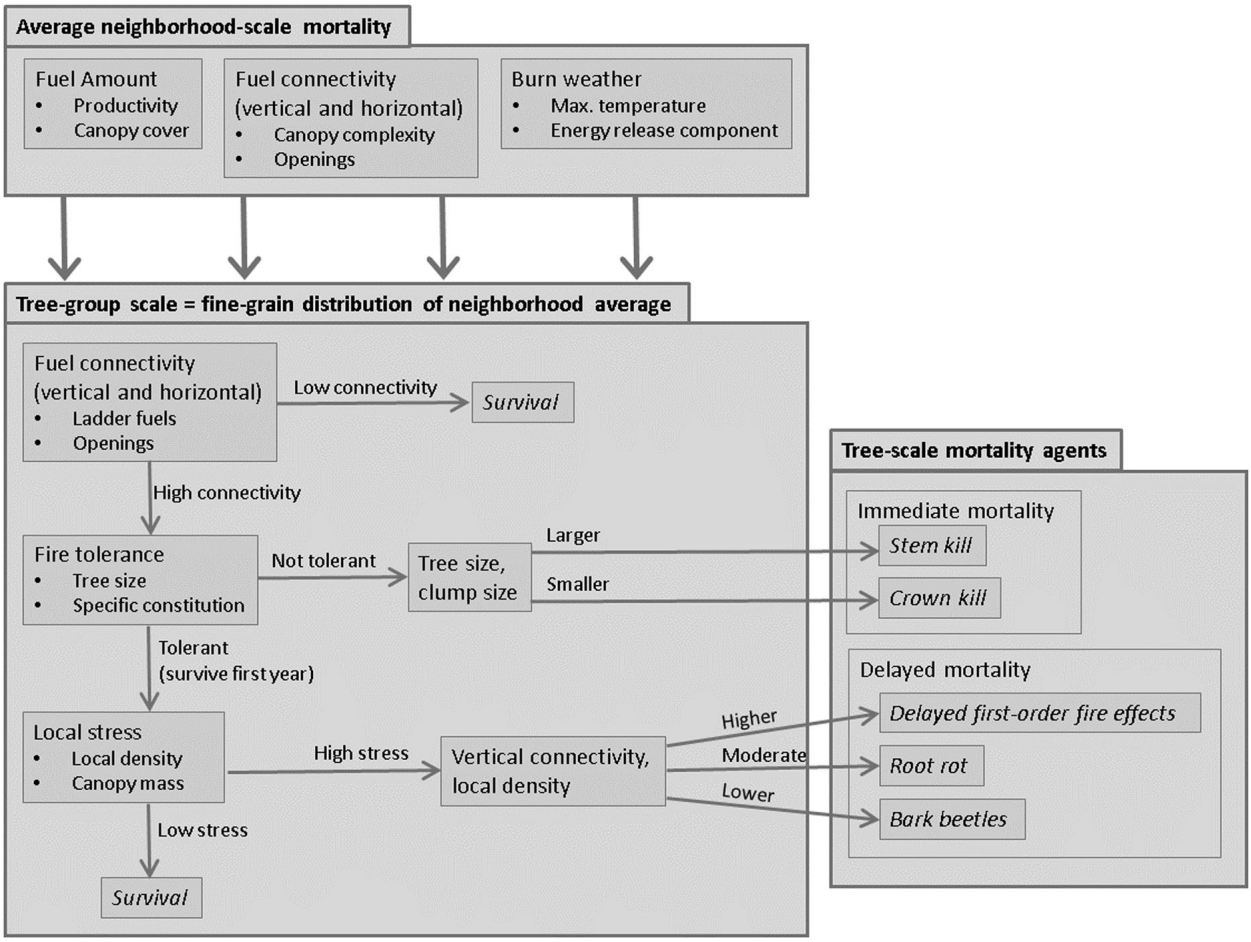

Fig. 9. Conceptual representation of study results. Post-fire tree mortality is driven from broader scales to finer scales, where fuel and burn weather attributes at the neighborhood scale determine the total amount of mortality and factors at the scale of small groups of trees determine the spatial distribution of that mortality. The process of post-fire mortality at the tree-group scale can be conceptualized as a series of filters. Fine-scale fuel connectivity determines a given tree group's risk of fire mortality. For tree groups with high fuel connectivity, fire tolerance determines first-year survival and local stresses determine longer-term survival. The actual mechanisms of death vary based on timing and fine-scale structure.

Question 3

Including cross-scale linkages between neighborhood-level and TAO-level models substantially improved model fits (Table 3). This aligns with the theoretical understanding of fire's landscape ecology, where different scales rest within a hierarchical structure with cross-scale interactions. The degree of improvement realized at the TAO scale was more than at the neighborhood scale,

suggesting that cross-scale interactive drivers of fire severity exert a stronger influence from broader to finer scales than the reverse. However, spatial configuration of fuels at the neighborhood scale was also an important driver: the model that included a cross-scale linkage but excluded water balance, burning weather, and topography metrics performed nearly as well as the model that included them. It appears that, rather than fine-scale effects integrating up to form a broad-scale result, the broad-scale conditions instead form the basic template that undergoes local modifications according to fine-scale conditions.

Table 3. Model assessment statistics for the four tested model formulations. The best statistic for each column is in bold italic face. Abbreviations: S = structure only, ST = structure + topography, SL = structure + cross-scale linkage, STL = structure + topography + cross-scale linkage. RMSE = root mean squared error; D_{sel} = posterior predictive loss function, where lower numbers represent a better and more parsimonious model fit; LPD = log predictive density, where higher (less negative) numbers represent a better and more parsimonious model fit.

Neighborhood scale			**RMSE (trees ha^{-1})**		
	Model	**D_{sel}**	**Immediate mortality**	**Delayed mortality**	**Total mortality**
	S	926699	78.7	63.4	89.4
	ST	426853	70.8	44.3	84.8
	SL	924992	76.8	63.4	89.4
	STL	***426432***	***70.1***	***43.9***	***84.4***

Tree-approximate object scale			**RMSE (n trees)**			
			In-sample		**Out-of-sample**	
	Model	**LPD**	**Immediate mortality**	**Delayed mortality**	**Immediate mortality**	**Delayed mortality**
	S	-5716	1.693	1.759	1.898	1.388
	ST	-5394	1.693	1.759	1.897	***1.387***
	SL	-4842	1.638	1.734	1.886	1.398
	STL	***-4793***	***1.613***	***1.706***	***1.885***	1.403

Question 4

For immediate mortalities, trees within taller TAOs and trees within larger clumps suffered less crown damage and more stem damage. Of delayed mortalities occurring 2-4 years post-fire, 35% had no indications of mortality agents other than fire damage and 71% of mortality factors in total were fire-related. Higher crown base heights shifted the balance of delayed mortality causes away from fire effects. The amount of fire-related mortality was higher in high-density local areas, indicating that recovery from first-order fire damage, even without subsequent stresses by beetles, pathogens, or mechanical damage, is density-dependent and specifically is counteracted by high local density.

Associations between fine-scale structure and non-fire delayed mortality agents took the form of tradeoffs between mortality dominated by pathogens and mortality dominated by beetles. Deep crowns and high TAO density were associated with more mortality due to pathogens, whereas the balance shifted toward beetle kill when crown bases were high and local density was low to moderate (<180 trees ha^{-1}).

Conclusions

We found that patterns of post-fire mortality are driven by multiple factors interacting across scales. A theory of cross-scale interactions has been developed for fire regimes but has not been described for fire effects within an individual fire. As fire moves contagiously across a landscape

its ultimate effects are determined by a complex of processes occurring at and interacting across multiple scales. This study represents a step in the development of the landscape ecology of fire and suggests that formalizing the hierarchical structure of landscapes in empirical models is a productive way to advance the ecological understanding of disturbance processes.

Mentoring Outcomes

This project partially supported two graduate students in their Ph.D. programs. Sean Medeiros Alexander Jeronimo received his Ph.D. from the University of Washington in 2018. He is now an owner of Resilient Forestry, LLC, a land management consulting company. Tucker James Furniss will receive his Ph.D. from Utah State University in 2021. He is now a post-doctoral scholar investigating landscape-level fire effects for the USFS PNW Research Station.

Departures from Proposed Activities

We exceeded our project objectives and deliverables (Table 6). The Covid-19 outbreak precluded our presenting and discussing results with Yosemite science and fire managers. The Yosemite Head of Science (Nicole Athearn, Ph.D.) and I agreed to do this as soon as practical with a public presentation at Yosemite and a tour of the study area with managers. We published our full datasets open access through the Utah State University libraries (Cansler et al. 2018, Macriss et al. 2019) instead of using the USFS databank. All data and metadata were published with a permanent DOI under the open-access Creative Commons Attribution 4.0 License after review by Utah State University digital librarians.

Science Delivery Activities

The two new datasets and one field and database manual generated in this project constitute another significant science delivery and are already generating external use and development of secondary science delivery products.

Synthesis and Conclusions

Key Publications

Lutz, J. A., A. J. Larson, and M. E. Swanson. 2018. Advancing fire science with large forest plots and a long-term multidisciplinary approach. *Fire* 1(1): 5. http://dx.doi.org/10.3390/fire1010005

Lutz, J. A, S. Struckman, T. J. Furniss, C. A. Cansler, S. J. Germain, L. L. Yocom, D. J. McAvoy, C. A. Kolden, A. M. S. Smith, M. E. Swanson, and A. J. Larson. 2020. Large-diameter trees dominate snag and surface biomass following reintroduced fire. *Ecological Processes* 9:41. https://doi.org/10.1186/s13717-020-00243-8

Cansler, C. A., M. E. Swanson, T. J. Furniss, A. J. Larson, and J. A. Lutz. 2019. Fuel dynamics after reintroduced fire in an old-growth Sierra Nevada mixed-conifer forest. *Fire Ecology* 15:16. https://doi.org/10.1186/s42408-019-0035-y

Key Findings

Large, spatially-explicit forest plots reveal a more ecologically nuanced understanding of fire effects (Lutz 2015, Lutz et al. 2018). The establishment of the Yosemite Forest Dynamics Plot, and subsequent burning by the Rim Fire, enabled us to leverage a decade of annual tree mortality measurements among tens of thousands of trees to evaluate fire science tools in novel ways. The post-fire research we conducted with this unique dataset is a powerful complement to previous studies based on more traditional sampling designs, making this body of research a critical contribution to the field of fire ecology.

It is often assumed that warmer climates increase post-fire mortality, but our research demonstrated the magnitude of this effect. Climate effects were pronounced for large-diameter trees which can be more susceptible to insects, and we documented a climate-related pulse in mortality in the years following the Rim Fire.

We found that the most widely used mortality model, FOFEM, may not be suitable to predict post-fire mortality of hardwood species or large-diameter trees. Background mortality agents (i.e., bark beetles) and dense tree neighborhoods can increase probability of mortality, and this can result in patches of elevated mortality. Spatial metrics can be incorporated into mortality models to improve accuracy.

Satellite-derived fire severity maps may reflect broad-scale patterns in severity but should not be treated as absolute truth. Uncertainty may be reduced by supplementing severity maps with field-based observations of fire effects.

Fuel deposition and consumption is extremely heterogeneous (Lutz et al. 2020), suggesting that fire planning may need to consider higher levels of sampling, and also that heavy fuel evolution (the transitions between trees, snags, and down woody debris) need more research focus.

Table 4. Deliverable products and delivery dates, both as listed in the original project proposal (left three columns) and as actually delivered (right column). PDFs of all peer-reviewed publications, including supplemental material, are attached at the end of this report. In author lists, bold typeface indicates project investigators and blue typeface indicates graduate students supported by this project.

Deliverable Type (see proposal instructions)	As Planned	Delivery Dates	As Delivered
Referred publication (target: *Ecological Applications*)	Journal article comparing predictive abilities of spatially explicit post-fire models of mortality with non-spatially explicit models.	July 2019	Furniss†, T. J., **A. J. Larson**, **V. R. Kane**, and **J. A. Lutz**. 2019. Multi-scale assessment of post-fire tree mortality models. *International Journal of Wildland Fire* 28(1): 46-61. https://doi.org/10.1071/WF18031 **Selected as Editor's Choice**
Refereed publication (target: *Remote Sensing of Environment*)	Journal article reporting the correlations between Landsat-derived fire severity indices, LiDAR-derived TAO metrics, and actual tree mortality.	July 2019	Furniss†, T. J., **V. R. Kane**, **A. J. Larson**, and **J. A. Lutz**. 2020. Detecting actual tree mortality with satellite-derived spectral indices and estimating landscape-level uncertainty. *Remote Sensing of Environment* 237: 111497. https://doi.org/10.1016/j.rse.2019.111497
			Furniss†, T. J., **A. J. Larson**, **V. R. Kane**, and **J. A. Lutz**. 2020. Wildfire and drought moderate the spatial elements of tree mortality. *Ecosphere* 11(8): e03214. https://doi.org/10.1002/ecs2.3214
			Lutz, J. A., S. Struckman, T. J. Furniss†, C. A. Cansler, S. J. Germain†, L. L. Yocom, D. J. McAvoy, C. A. Kolden, A. M. S. Smith, M. E. Swanson, and **A. J. Larson**. 2020. Large-diameter trees dominate snag and surface biomass following reintroduced fire. *Ecological Processes* 9:41. https://doi.org/10.1186/s13717-020-00243-8
			Jeronimo†, S. M. A., **J. A. Lutz**, **V. R. Kane**, **A. J. Larson**, and J. F. Franklin. 2020. Burn weather and three-dimensional fuel structure determine post-fire tree mortality. *Landscape Ecology* 35: 859-878 https://doi.org/10.1007/s10980-020-00983-0
			Cansler, C. A., M. E. Swanson, T. J. Furniss†, **A. J. Larson**, and **J. A. Lutz**. 2019. Fuel dynamics after reintroduced fire in an old-growth Sierra Nevada mixed-conifer forest. *Fire Ecology* 15:16. https://doi.org/10.1186/s42408-019-0035-y
			Lutz, J. A., **A. J. Larson**, and M. E. Swanson. 2018. Advancing fire science with large forest plots and a long-term multidisciplinary approach. *Fire* 1(1): 5. http://dx.doi.org/10.3390/fire1010005
Non-refereed	A one page, two sided laminated description	May 2017	Completed, March 2020 (attached to end of report)

publication	of the research and preliminary findings for Park Service use		
Non-refereed publication	A field manual for the validation process.	May 2019	Included in Jeronimo *et al.* 2020.
			Janík, D., K. Král, D. Adam, T. Vrška, and **J. A. Lutz**. 2018. ForestGEO Dead Wood Census Protocol. Data Set 76. https://doi.org/10.26078/vcdr-y089
Poster (2)	Target presentation venues: Association of Fire Ecologists and Ecological Society of America.	September 2017 July 2018	Presentations substituted for posters
Presentations (4)	Target presentation venues: Yosemite Science Forum, Restoring the West, American Geophysical Union.	2018	Nine presentations (PDFs of presentations available at http://yfdp.org/Fire.html
			Furniss†, T. J. and **J. A. Lutz**. 2020. Big plots, big trees, and big fires: Enhancing our ecological understanding of fire effects with unprecedented field data. Ecological Society of America Annual Meeting. Salt Lake City, UT. August 5.
			Furniss†, T. J. and **J. A. Lutz**. Interactive effects of drought, fire, and bark beetles on tree mortality in the Sierra Nevada, California. Wildland Resources Dept. Graduate Research Seminar. Logan, UT. April 12, 2019.
			Furniss†, T. J., S. M. A. Jeronimo, **V. R. Kane**, **A. J. Larson**, and **J. A. Lutz**. Quantifying uncertainty in satellite-derived fire severity using actual tree mortality. International Association for Landscape Ecology 2019 Annual Meeting. Fort Collins, CO. April 8, 2019.
			Furniss†, T. J., **A. J. Larson**, **V. R. Kane**, and **J. A. Lutz**. Advancing fire science with unprecedented forest demography data. Rocky Mountain Research Station Fire Lab Seminar Series 2018-2019. Missoula, MT. April 4, 2019.
			Jeronimo†, S. M. A. Three-dimensional fuel structure and cross-scale interactions drive post-fire tree mortality. International Association for Landscape Ecology 2019 Annual Meeting. Fort Collins, CO. April 8, 2019.
			Furniss†, T. J., **A. J. Larson**, **V. R. Kane**, and **J. A. Lutz**. Spatial elements of fire-related mortality. Intermountain Society of American Foresters Annual Meeting. Logan, UT. March 29, 2019.
			Jeronimo†, S. M. A. Fire and forest structure in the Sierra Nevada mixed-conifer zone. Rocky Mountain Research Station Fire Lab Seminar Series 2018-2019. Missoula, MT. February 14, 2019.

			Jeronimo†, S. M. A., T. J. Furniss†, **V. R. Kane**, **A. J. Larson**, and **J. A. Lutz**. New approaches to fire mortality modelling incorporating spatially explicit multi-scale structure. Fire Continuum Conference. Missoula, MT. May 24, 2018.
			Furniss†, T. J., and **J. A. Lutz**. Improving fire mortality models for Sierra Nevada mixed-conifer forests. Utah State University Graduate Research Symposium. Logan, UT. April 14, 2017.
Training session	We will present our work in a multi-agency webinar	2018	Deferred until late 2021 at Yosemite
Training session	We will present our research results at a management-oriented workshop at Yosemite National Park.	May 2019	Deferred until late 2021 at Yosemite
Website	The existing project website (http://yfdp.org) will be enhanced with project results and data.	September 2016 - July 2019	Completed: http://yfdp.org/Fire.html
Graduate thesis	Working title: Spatial correlates of post-fire tree mortality in a Sierra Nevada mixed-conifer forest.	May 2019	Jeronimo†, S. M. A. 2018. Restoring forest resilience in the Sierra Nevada mixed-conifer zone, with a focus on measuring spatial patterns of trees using airbourne lidar. Dissertation. University of Washington, Seattle, Washington, August, 2018.
			Furniss†, T. J. 2021. Big fires, big trees, and big plots: Enhancing our ecological understanding of fire with unprecedented field data. Dissertation. Utah State University, Logan, Utah. Expected, 2021.
	Field validation plot dataset and metadata		Macriss, N., T. J. Furniss†, S. M. A. Jeronimo†, E. L. Crowley, O. W. Germain, S. J. Germain†, **V. R. Kane**, **A. J. Larson**, and **J. A. Lutz**. 2019. Data for tree mortality calibration of satellite and LiDAR-derived fire severity estimates. Utah State University. Data Set 63. https://doi.org/10.26078/jsz1-3980
	Surface fuel dataset and metadata		Cansler, C. A., M. E. Swanson, T. J. Furniss†, **A. J. Larson**, and **J. A. Lutz**. 2018. Data for pre-fire and post-fire surface fuel loading in a Sierra Nevada mixed-conifer forest. Utah State University. Data Set 51. https://doi.org/10.15142/T3G93X

†Graduate student

Literature Cited

Anderson-Teixeira, K. J., S. J. Davies, A. J. Larson, J. A. Lutz, and 85 co-authors. 2015. CTFS-ForestGEO: A worldwide network monitoring forests in an era of global change. Global Change Biology 21(2): 528-549.

Baddeley, A., and T. Turner. 2005. Spatstat: an R package for analyzing spatial point patterns. Journal of Statistical Software 12(6): 1-42.

Baig, M. HA, L. Zhang, T. Shuai, Q. Tong Derivation of a tasselled cap transformation based on Landsat 8 at-satellite reflectance Remote Sens. Lett., 5 (2014), pp. 423-431

Barbosa, P. M., D. Stroppiana, J.-M. Grégoire, and J. M. Cardoso Pereira. 1999. An assessment of vegetation fire in Africa (1981-1991): burned areas, burned biomass, and atmospheric emissions. Global Biogeochemical Cycles 13: 933-950.

Barth, M. A. F., A. J. Larson, and J. A. Lutz. 2015. Use of a forest reconstruction model to assess changes to Sierra Nevada mixed-conifer forest during the fire suppression era. Forest Ecology and Management 354: 104-118.

Belote, R. T., A. J. Larson, and M. S. Dietz. 2015. Tree survival scales to community-level effects following mixed-severity fire in a mixed-conifer forest. For. Ecology and Management 353: 221-231.

Cansler, C. A., M. E. Swanson, T. J. Furniss, A. J. Larson, and J. A. Lutz. 2018. Data for pre-fire and post-fire surface fuel loading in a Sierra Nevada mixed-conifer forest. Utah State University. Data Set 51. https://doi.org/10.15142/T3G93X

Cansler, C. A., M. E. Swanson, T. J. Furniss, A. J. Larson, and J. A. Lutz. 2019. Fuel dynamics after reintroduced fire in an old-growth Sierra Nevada mixed-conifer forest. *Fire Ecology* 15:16. https://doi.org/10.1186/s42408-019-0035-y

Clyatt, K. A., J. S. Crotteau, M. S. Schaedel, H. L. Wiggins, H. Kelley, D. J. Churchill, and A. J. Larson. 2015. Historical spatial patterns and contemporary tree mortality in dry mixed-conifer forests. Forest Ecology and Management 361: 23-37.

Condit, R. 1998. Tropical Forest Census Plots. Springer-Verlag. Berlin.

Condit, R., S. Lao, A. Singh, S. Esufali, and S. Dolins. 2014. Data and database standards for permanent forest plots in a global network. Forest Ecology and Management 316:21-31.

Contreras, M.A., D. Affleck, and W. Chung. 2011. Evaluating tree competition indices as predictors of basal area increment in western Montana forests. Forest Ecology and Management 262: 1939-1949

Das, A, J. Battles, N. L. Stephenson, and P. J. van Mantgem. 2011. The contribution of competition to tree mortality in old-growth coniferous forests. Forest Ecology and Management 261:1203-1213.

Eidenshink, J., B. Schwind, K. Brewer, Z. Zhu, B. Quale, and S. Howard. 2007. A project for monitoring trends in burn severity. Fire Ecology 3(2): 53-67.

Epting, J., D. Verbyla, and B. Sorbel 2005. Evaluation of remotely sensed indices for assessing burn severity in interior Alaska using Landsat TM and ETM+ Remote Sensing of Environment 96: 328-339.

Furniss, T. J., A. J. Larson, V. R. Kane, and J. A. Lutz. 2020. Wildfire and drought moderate the spatial elements of tree mortality. *Ecosphere*. 11(8): e03214. https://doi.org/10.1002/ecs2.3214

Furniss, T. J., A. J. Larson, V. R. Kane, and J. A. Lutz. 2019. Multi-scale assessment of post-fire tree mortality models. *International Journal of Wildland Fire* 28(1): 46-61. https://doi.org/10.1071/WF18031

Gao, B. 1996. NDWI—a normalized difference water index for remote sensing of vegetation liquid water from space. Remote Sensing of Environment 58: 257-266.

Hood, S. M., C. W. McHugh, K. C. Ryan, E. Reinhardt, and S. L. Smith. 2007. Evaluation of a post-fire tree mortality model for western USA conifers. International Journal of Wildland Fire 16: 679-689.

Hood, S. M., S. L. Smith, and D. R. Cluck. 2010. Predicting mortality for five California conifers following wildfire. Forest Ecology and Management 260: 750-762.

Hosmer, D. W., S. Lemeshow, and R. X. Sturdivant. 2013. Applied logistic regression. Third edition. John Wiley and Sons. 528 pp.

Huete, A. 1988. A soil-adjusted vegetation index (SAVI) Remote Sensing of Environment 25: 295-309.

Jeronimo, S.M.A. 2015. LiDAR individual tree detection for assessing structurally diverse forest landscapes. Master's Thesis, University of Washington, Seattle, Washington.

Jeronimo, S. M. A., J. A. Lutz, V. R. Kane, A. J. Larson, and J. F. Franklin. 2020. Burn weather and three-dimensional fuel structure determine post-fire tree mortality. *Landscape Ecology* 35: 859-878. https://doi.org/10.1007/s10980-020-00983-0

Kane, V. R., C. A. Cansler, N. A. Povak, J. T. Kane, R. J. McGaughey, J. A. Lutz, D. J. Churchill, and M. P. North. 2015b. Mixed severity fire effects within the Rim fire: Relative importance of local climate, fire weather, topography, and forest structure. Forest Ecology and Management 358: 62-79.

Kane, V. R., J. A. Lutz, C. A. Cansler, N. A. Povak, D. Churchill, D. F. Smith, J. T. Kane, and M. P. North. 2015a. Water balance and topography predict fire and forest structure patterns. Forest Ecology and Management 338: 1-13.

Kane, V. R., M. North, J. A. Lutz, D. Churchill, S. L. Roberts, D. F. Smith, R. J. McGaughey, J. T. Kane, and M. L. Brooks. 2014. Assessing fire-mediated change to forest spatial structure using a fusion of Landsat and airborne LiDAR data in Yosemite National Park. Rem. Sens. Env. 151: 89-101.

Kaartinen, H., J. Hyyppä, X. Yu, M. Vastaranta, H. Hyyppä, A. Kukko, M. Holopainen, C. Heipke, M. Hirschmugl, F. Morsdorf, E. Næsset, J. Pitkänen, S. Popescu, S. Solberg, B.M. Wolf, and J.-C. Wu. 2012. An International Comparison of Individual Tree Detection and Extraction Using Airborne Laser Scanning. Remote Sensing 4: 950-974.

Key, C. H., and N. C. Benson. 2006. Landscape assessment: ground measure of severity, the Composite Burn Index, and remote sensing of severity, the Normalized Burn Ratio. Pages LA1-LA55 in FIREMONL fire effects monitoring and inventory system. D. C. Lutes, R. E. Keane, J. F. Carratti, C. H. Key, N. C. Benson, S. Sutherland, and L. J. Gangi. USDA Forest Service RMRS-GTR-164CD.

Kolden, C. A., J. A. Lutz, C. H. Key, J. T. Kane, and J. W. van Wagtendonk. 2012. Mapped versus actual burned area within fire perimeters: characterizing the unburned. For. Ecol. Manage. 286: 38-47.

Kushla, J. D., and W. J. Ripple. 1998. Assessing wildfire effects with Landsat thematic mapper data. International Journal of Remote Sensing 19: 2493-2507.

Larson, A. J., J. A. Lutz, D. C. Donato, J. A. Freund, M. E. Swanson, J. HilleRisLambers, D. G. Sprugel, and J. F. Franklin. 2015. Spatial aspects of tree mortality strongly differ between

young and old-growth forests. Ecology. doi: http://dx.doi.org/10.1890/15-0628.1
Lutes, D. C. 2014. FOFEM 6.1 First Order Fire Effects Model User Guide. Fire and Aviation Management, Rocky Mountain Research Station.
Lutz, J. A. 2015. The evolution of long-term data for forestry: large temperate research plots in an era of global change. Northwest Science 89(3).
Lutz, J. A., A. J. Larson, T. J. Furniss, J. A. Freund, M. E. Swanson, D. C. Donato, K. J. Bible, J. Chen, and J. F. Franklin. 2014. Spatially non-random tree mortality and ingrowth maintain equilibrium pattern in an old-growth Pseudotsuga-Tsuga forest. Ecology 95(8): 2047-2054.
Lutz, J. A., A. J. Larson, J. A. Freund, M. E. Swanson, K. J. Bible. 2013. The importance of large-diameter trees to forest structural heterogeneity. PLoS ONE 8(12): e82784.
Lutz, J. A., A. J. Larson, M. E. Swanson, J. A. Freund. 2012. Ecological importance of large-diameter trees in a temperate mixed-conifer forest. PLoS ONE 7(5): e36131.
Lutz, J. A., C. H. Key, C. A. Kolden, J. T. Kane, and J. W. van Wagtendonk. 2011. Fire frequency, area burned, and severity: A quantitative approach to defining a normal fire year. Fire Ecology 7(2): 51-65.
Lutz, J. A., A. J. Larson, and M. E. Swanson. 2018. Advancing fire science with large forest plots and a long-term multidisciplinary approach. *Fire* 1(1): 5. http://dx.doi.org/10.3390/fire1010005
Lutz, J. A, S. Struckman, T. J. Furniss, C. A. Cansler, S. J. Germain, L. L. Yocom, D. J. McAvoy, C. A. Kolden, A. M. S. Smith, M. E. Swanson, and A. J. Larson. 2020. Large-diameter trees dominate snag and surface biomass following reintroduced fire. *Ecological Processes* 9:41. https://doi.org/10.1186/s13717-020-00243-8
Macriss, N., T. J. Furniss, S. M. A. Jeronimo, E. L. Crowley, O. W. Germain, S. J. Germain, V. R. Kane, A. J. Larson, and J. A. Lutz. 2019. Data for tree mortality calibration of satellite and LiDAR-derived fire severity estimates. Utah State University. Data Set 63. https://doi.org/10.26078/jsz1-3980
McCarley, T. R., C. A. Kolden, N. M. Vaillant, A. T. Hudak, A. M. S. Smith, and J. Kreitler. 2017. Landscape-scale quantification of fire-induced change in canopy cover following mountain pine beetle outbreak and timber harvest. Forest Ecology and Management 391: 164-175.
McCarley, T. R., A. M. S. Smith, C. A. Kolden, and J. Kreitler. 2018. Evaluating the mid-infrared bi-spectral index for improved assessment of low-severity fire effects in a conifer forest. International Journal of Wildland Fire 27: 407-412.
Meddens, A. J. H., C. A. Kolden, and J. A. Lutz. 2016. Detecting unburned areas within wildfire perimeters using Landsat and ancillary data across the northwestern United States. Remote Sensing of Environment 186: 275-285.
Miller, J. D., and A. E. Thode. 2007. Quantifying burn severity in a heterogeneous landscape with a relative version of the delta Normalized Burn Ratio (dNBR). Rem. Sens. Env. 109: 66-80.
Negrón, J. F., and J. B. Popp. 2004. Probability of ponderosa pine infestation by mountain pine beetle in the Colorado Front Range. Forest Ecology and Management 191: 17-27.
Olano, J. M., N. A. Laskurain, A. Escudero, and M. De La Cruz. 2009. Why and where do adult trees die in a young secondary temperate forest? The role of neighborhood. Annals of Forest Science 66: 105.
Oliver, C. D., and B. C. Larson. 1996. Forest Stand Dynamics. John Wiley and Sons, New York. 544 pp.

Parks, S. A., G. K. Dillon, and C. Miller. 2014. A new metric for quantifying burn severity: the Relativized Burn Ratio. Remote Sensing 6: 1827-1844.

Richardson, J. J., and L. M. Moskal. 2011. Strengths and limitations of assessing forest density and spatial configuration with aerial LiDAR. Remote Sensing of Environment 115: 2640-2651.

Robin, X., N. Turck, A. Hainard, N. Tiberti, F. Lisacek, J-C. Sanchez, and M. Müller. 2011. pROC: an open-source package for R and S+ to analyze and compare ROC curves. BMC Bioinformatics 12:77.

Rouse, W., and R. H. Haas. 1974. Monitoring Vegetation Systems in the Great Plains with ERTS, vol. 9.

Ryan, K. C., and E. D. Reinhardt. 1988. Predicting post-fire mortality of sever western conifers. Canadian Journal of Forest Research 18: 1291-1297.

Smith, A. M. S., N. A. Drake, M. J. Wooster, A. T. Hudak, Z. A. Holden, and C. J. Gibbons. 2007. Production of Landsat ETM+ reference imagery of burned areas within Southern African savannahs: comparison of methods and application to MODIS. International Journal of Remote Sensing 28: 2753-2775.

Stavros, E. N., Z. Tane, V. R. Kane, S. Veraverbeke, R. J. McGaughey, J. A. Lutz, and C. Ramirez. In Revision. Unprecedented remote sensing data from before and after the California King and Rim megafires. Nature Scientific Data.

Storey, J., M. Choate, and K. Lee. 2014. Landsat 8 Operational Land Imager on-orbit geometric calibration and performance. Remote Sensing 6(11): 11127-11152.

Thies, W. G., and D. J. Westlind. 2012. Validating the Malheur model for predicting ponderosa pine post-fire mortality using 24 fires in the Pacific Northwest, USA. Int. Journal of Wildland Fire 21: 572-582.

Trigg, S, and S. Flasse. 2001. An evaluation of different bi-spectral spaces for discriminating burned shrub-savannah. International Journal of Remote Sensing 22: 2641-2647.

Tucker, C. J. 1979. Red and photographic infrared linear combination for monitoring vegetation. Remote Sensing of Environment 8(2): 127-150.

USDI National Park Service. 2003. Fire Monitoring Handbook. Boise (ID): Fire Management Program Center, National Interagency Fire Center. 274 pp.

USGS LANDSAT 8 (L8) Data Users Handbook Version 2.0 U.S. Geological Survey, Department of the Interior. Sioux Falls, South Dakota, USA (2016), p. 106

van Mantgem, P. J., J. C. B. Nesmith, M. Keifer, E. E. Knapp, A. Flint, and L. Flint. 2013. Climatic stress increases forest fire severity across the western United States. Ecology Letters ele.12151.

van Wagtendonk, J. W., and J. A. Lutz. 2007. Fire regime attributes of wildland fires in Yosemite National Park, USA. Fire Ecology 3(2): 34-52.

Vogelmann, J. E. 1990. Comparison between two vegetation indices for measuring different types of forest damage in the north-eastern United States. International Journal of Remote Sensing 11: 2281-2297.

Wilson, E. H., and S. A. Sader. 2002. Detection of forest harvest type using multiple dates of Landsat TM imagery. Remote Sensing of Environment 80: 385-396.

Yu, H., T. Wiegand, A. Yang, and L. Ci. 2009. The impact of fire and density-dependent mortality on the spatial patterns of a pine forest in the Hulun Buir sandland, Inner Mongolia, China. Forest Ecology and Management 257: 2098-2107.

Appendices

Appendix A: Contact Information for Key Project Personnel

Appendix B: List of Completed Scientific Publications and Science Delivery Products:

Appendix C: Metadata

Appendix D: Furniss, T. J., A. J. Larson, V. R. Kane, and J. A. Lutz. 2019. Multi-scale assessment of post-fire tree mortality models. *International Journal of Wildland Fire* 28: 46-61. *Uploaded to JSFP website, including supplemental information and code.*

Appendix E: Furniss, T. J., V. R. Kane, A. J. Larson, and J. A. Lutz. 2020. Detecting tree mortality with Landsat-derived spectral indices: Improving ecological accuracy by examining uncertainty. *Remote Sensing of Environment* 237: 111497. *Uploaded to JSFP website, including supplemental information.*

Appendix F: Furniss, T. J., A. J. Larson, V. R. Kane, and J. A. Lutz. 2020. Wildfire and drought moderate the spatial elements of tree mortality. *Ecosphere* 11(8): e03214. *Uploaded to JSFP website, including supplemental information and field data sheet.*

Appendix G: Lutz, J. A., S. Struckman, T. J. Furniss, C. Alina Cansler, S. J. Germain, L. L. Yocum, D. J. McAvoy, C. A. Kolden, A. M. S. Smith, M. E. Swanson, and A. J. Larson. 2020. Large-diameter trees dominate snag and surface biomass following reintroduced fire. *Ecological Processes* 9: 41. *Uploaded to JSFP website, including supplemental information.*

Appendix H: Jeronimo, S. M. A., J. A. Lutz, V. R. Kane, A. J. Larson, and J. F. Franklin. 2020. Burn weather and three-dimensional fuel structure determine post-fire tree mortality. *Landscape Ecology* 38: 859-878. *Uploaded to JSFP website, including supplemental information and plot metadata.*

Appendix I: Cansler, C. A., M. E. Swanson, T. J. Furniss, A. J. Larson, and J. A. Lutz. 2019. Fuel dynamics after reintroduced fire in an old-growth Sierra Nevada mixed-conifer forest. *Fire Ecology* 15: 16. *Uploaded to JSFP website, including supplemental information.*

Appendix J: Lutz, J. A., A. J. Larson, and M. E. Swanson. 2018. Advancing fire science with large forest plots and a long-term multidisciplinary approach. *Fire* 1: 5. *Uploaded to JSFP website.*

Appendix K: Janík, D., K Král, D, Adam, T. Vrška, and J. A. Lutz. 2018. ForestGEO Dead Wood Census Protocol. Utah State University Dataset 76. *Uploaded to JSFP website, including field methods and data dictionary.*